

# Interactions between hosts affect virus competition mechanism within an infectious strain

Javier López-Pedrares<sup>a,b,c</sup>, M. Elena Vázquez-Cendón<sup>a,c</sup>, Alberto P. Muñuzuri<sup>a,b,\*</sup>

<sup>a</sup> Galician Center for Mathematical Research and Technology (CITMAga), 15782 Santiago de Compostela, Spain

<sup>b</sup> Group of Nonlinear Physics, Universidade de Santiago de Compostela, 15782 Santiago de Compostela, Spain

<sup>c</sup> Department of Applied Mathematics, Universidade de Santiago de Compostela, 15782 Santiago de Compostela, Spain

## ARTICLE INFO

### Keywords:

Competition model  
Epidemiological model  
Ordinary differential equations  
Virus  
Pandemic  
Complex network

## ABSTRACT

Competition of different viruses in a common strain usually results in one variant dominating over all others and eventually suppressing them, following the Principle of Competitive Exclusion. Viruses host in larger animals and they spread to others via the interactions between the hosts. In the present communication, we focus on the role played by the interacting hosts in determining the evolutionary path of a strain. Simple mathematical models are considered to model the evolution of the strain as well as to model the spread of the disease. We observe that the structure of the interactions between hosts influences the evolutionary mechanism as well as the spread of the disease.

## 1. Introduction

The spread of a contagious disease is a complicated phenomenon that has been extensively studied in the recent times [1–3]. Many mathematical models have been tested considering complicated scenarios and their validity has been demonstrated in practical situations [4–6]. The problem becomes more complex if we take into account the different microorganisms that actually are contained in the strain and are competing for the same resources (the host). This is especially relevant when long term processes are considered.

The competitive exclusion principle [7] says that two or more species cannot coexist if they compete for identical resources. The different viruses contained in a strain that has infected a host are also competing for the same resources. As a general principle, one can consider that, if the host lives long enough, the viruses within that particular strain will endure this competition process resulting in the survival of the more suited virus and the extinction of all others in the strain.

In real life, the spread of a disease is much more complicated than it is described in this scenario as the potential hosts interact between themselves favoring the spread of the disease and their natural defenses fight the disease killing all microorganisms in the strain. Thus, we can identify at least three mechanisms simultaneously acting, the spread of a given virus strain, the competition between the different viruses in the strain and the interactions between the potential hosts. Although there

are extensive literature modelling the spread of diseases [8–10] and some models also describe the competition of similar species [11,12]. The role played by the interactions between the potential hosts has not been fully analyzed [13].

The present manuscript focuses on the role played by the potential hosts interactions on the evolution of the disease and its spread. Complex networks can be used to describe the interactions between hosts and are susceptible to play a key role in viral evolution. We study the possible scenarios that appear when the network topology is modified. Historically and considering humans as the potential hosts, the interaction networks have changed dramatically [14,15]. Centuries ago, individuals were connected only to others nearby, but today we are connected to people from all over the planet following a completely different connections network. Different scenarios can be modelled using different topologies of the complex networks. There are differences between overcrowded cities and remote villages. The connection networks changed dramatically during the last decades and, consequently, the viral transmission is also expected to behave differently.

The paper is organized as follows. In the methods section we present the different models describing the virus competition within a host on the one hand and, in the other, the model describing the spread of the disease among the potential hosts. This section also contains information of the different networks describing the interaction between potential hosts. The numerical solution of the problem is presented in the

\* Corresponding author at: Galician Center for Mathematical Research and Technology (CITMAga), 15782 Santiago de Compostela, Spain.

E-mail address: [alberto.perez.munuzuri@usc.es](mailto:alberto.perez.munuzuri@usc.es) (A.P. Muñuzuri).

results. The final section is the discussion and conclusions.

## 2. Methods

### 2.1. Virus competition model

We considered a strain of viruses and phenotypically characterized them, i.e., we use the exhibited features characterizing each of them rather than their genome. We identify the following parameters that determine each virus in the strain;  $r$  is its reproduction rate,  $k$  is the competitive rate (its meaning will be clearer once the competition model is introduced below),  $p_{inf}$  measures the probability to infect an individual,  $t_{sick}$  is the infection latency time and  $t_{reinf}$  is the minimum time to have a reinfection. This set of five parameters will be specific for each virus in the strain.

The next step is to consider how the competition process develops. The simplest scheme is based on the Lotka-Volterra equations [16]. Let us call  $n$  the number of different viruses contained in a given strain, each characterized by a particular set of the five parameters that we already introduced. The total amount of each virus can be described by the following equation [17]

$$\frac{dV_i(t)}{dt} = r_i \left( 1 - \frac{\sum_{j=1}^n V_j(t)}{k_i} \right) V_i(t) \quad (1)$$

where  $V_i(t)$  is the density of the  $i$ -th virus at time  $t$ , with  $i = 1, \dots, n$ . Note that the subindex  $i$  refers to the  $i$ -th virus in the strain. The physical meaning of the parameters  $k$  and  $r$  becomes apparent in the context of the Lotka-Volterra equation.  $r_i$  is the reproductive rate of the  $i$ -th virus and  $k_i$  measures the competitions of the  $i$ -th virus with the others. The parameter  $k_i$  also describes the carrying capacity [18] of the host. In biology, more specifically in virology, the carrying capacity is the maximum viral population that the host can support in a certain instant of time. This model, without any further modification, can be easily integrated and the results are shown in the Supplementary Material.

### 2.2. Networks describing the interactions between potential hosts

The purpose of this manuscript is to evaluate the effect of the interactions between the potential hosts on the evolution of the virus competition and the disease spread. These interactions constitute a network whose nodes are the individuals (potential hosts) and the links represent the relationship between two individuals that may, eventually, result in contagion. Mathematically this is given by the adjacency matrix

$$A_{ij} = \begin{cases} 1 & \text{if nodes } i, j \text{ are connected (individual } i \text{ interacts with } j) \\ 0 & \text{if nodes } i, j \text{ are not connected (individual } i \text{ does not interact with } j) \end{cases} \quad (2)$$

Note that the adjacency matrix is symmetric by construction due to the symmetry of our problem. Different network structures are considered along this manuscript trying to mimic different experimental conditions. In particular, three topologies for the adjacency matrix are considered; random networks, small world (Watts-Strogatz) and scale free (Barabasi-Albert) [19–21]. Each topology describes different ways to interact the hosts. In a random network all individuals have the same connectivity, i.e. all are connected with the same number of other nodes that are chosen randomly among all the possible nodes. In a Watts-Strogatz network each node is connected with its closest neighbors plus some distant nodes that are chosen randomly with a given probability ( $p$ ). Depending on this probability, the network becomes diffusive for  $p = 0$  (there are only interactions with the closest neighbors as it was the case during pandemics in ancient times). Increasing  $p$  makes more probable interactions with distant individuals corresponding with a historical moment when communications become significant.  $p = 1$  corresponds with a random network again with a very high connectivity.

A scale-free network describes a highly industrial society where some individual display a very large connectivity while the majority present a moderate connectivity. The details of these networks are in the Supplementary Material.

For the simulations presented in this manuscript, we considered networks with 1000 nodes (potential hosts). With an average connectivity that depends on the particular type of network and situation analyzed.

### 2.3. Epidemiological model

The epidemiological model considered is based on the classic SIR model [21–29] and considers three different states for the population: susceptible (S), infected (I) and recovered individuals (R) with the transitions as sketched in Fig. 1a. Note that we consider that after some time the recovered may become susceptible again. This model has been extensively analyzed in the previous literature [30–32].  $\beta$  describes the probability of infection,  $\gamma$  is the probability to recover and  $\delta$  is the reinfection rate. Note that as we are considering a network of potential hosts, a non-infected node can only be infected if it is connected with an infected one (i.e., the adjacency matrix element for nodes  $i$  and  $j$ ,  $A_{ij}$  equals one).

This model becomes more complex in our case as the infections are given by a strain of multiple viruses that are competing among themselves following eq. (1). Each virus has a different probability of infection, recovery and reinfection that are determined by the set of properties describing each virus as introduced in the next subsection. We assume that the probability to infect is the larger of the strain and the characteristic times to recover and reinfect are also the larger. We also assume that when a node is infected, the whole strain as it was in the original host is transferred to the newly infected host.

### 2.4. Full model

All the components described above are integrated in a single model presented in the scheme in Fig. 1b. The epidemic model describes the dynamics of the disease, the host mobility network (given by the adjacency matrix) accounts for the interactions between potential hosts that may result in contagious and spread of the disease. The final element is the virus competition model that considers that a full strain of viruses with different phenotypes is present in each infected host. Now, not only the disease is evolving with time but also the nature of the strain causing the epidemic wave.

The network is initialized setting an initial number of nodes as infected while the rest are in the susceptible state and then, the simulation starts. At each time step, the chance that each infected individual spreads the disease to each of its susceptible connections is evaluated by means of a Monte Carlo method [33]. Then, the probability for each infected individual to recover is evaluated at the end of the time step in the same manner. After each time step, the virus competition model, Eq. (1), is numerically integrated using an explicit 4th order Runge-Kutta method. This process is repeated until the pool of infected individuals has decreased to zero or the virus strain has evolved into a single-virus strain.

The parameters controlling our model are the five parameters that describe phenotypically the initial set of viruses ( $r_i, k_i, p_{inf_i}, t_{sick_i}$  and  $t_{reinf_i}$ ). Two variables are recorded for each numerical simulation, the mean reinfection period that will be denoted by  $T_{wave}$  and the time to reach dominance of a single virus denoted by  $t_{fin}$ . Note that each virus in the strain has different values of the characteristic parameters. We consider a strain that initially is composed by  $n = 500$  different viruses. The actual values for these parameters are randomly taken from a uniform distribution following,

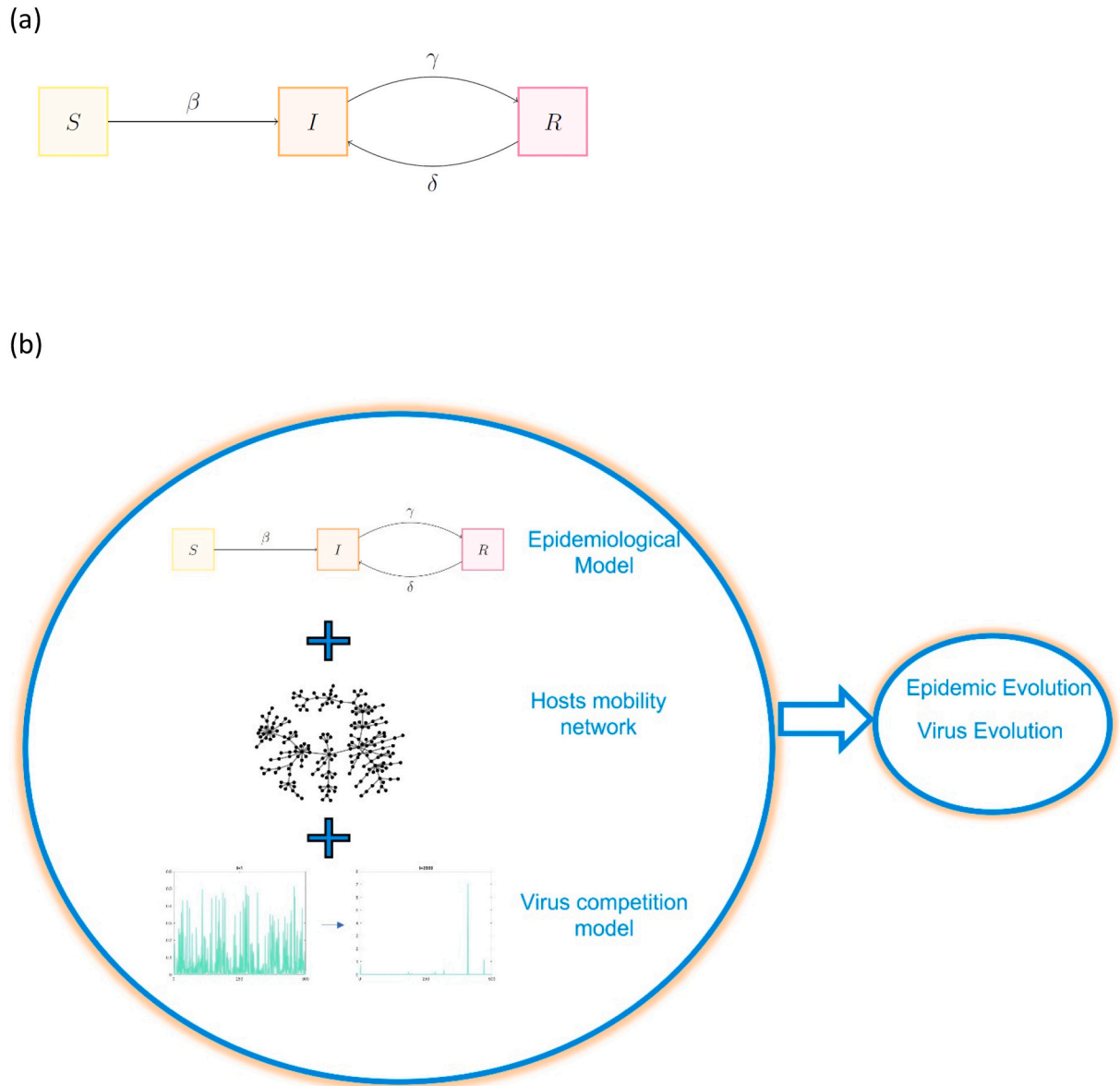


**Fig. 1.** Model schemes. (a) Scheme of the SIR model with reinfection. (b) Scheme integrating all the parts of the model including virus competition and SIR-like propagation in a complex network of potential hosts.

$$\begin{aligned}
 r_i &= r_{min} + \alpha_i(r_{max} - r_{min}) \\
 k_i &= k_{min} + \beta_i(k_{max} - k_{min}) \\
 p_{inf_i} &= p_{inf_{min}} + \gamma_i(p_{inf_{max}} - p_{inf_{min}}) \\
 t_{sick_i} &= t_{sick_{min}} + \delta_i(t_{sick_{max}} - t_{sick_{min}}) \\
 t_{reinf_i} &= t_{reinf_{min}} + \lambda_i(t_{reinf_{max}} - t_{reinf_{min}})
 \end{aligned}
 \tag{3}$$

with  $i = 1, \dots, n$  and  $\alpha_i, \beta_i, \gamma_i, \delta_i$  and  $\lambda_i$  are random numbers from a uniform distribution in the interval  $[0, 1)$ . The maximum and minimum values for each parameter are in Table 1. These values were chosen, after multiple tries, in order to guarantee the existence of successive epidemic waves

**Table 1**  
Range of values of the model parameters.

	$r$	$k$	$p_{inf}$	$t_{sick}$	$t_{reinf}$
min	0.1	0.5	0.001	10	400
max	8	10	0.009	20	500

that allowed long time observation of the virus strain.

Note that stochasticity is always present in the values of the parameters and the election of the first infected cases, thus, each simulation was run a hundred times in order to gain statistical significance.

### 3. Results

We performed extensive simulations following the protocol described in the previous section. A typical simulation is presented in Fig. 2 for very long computational times (around 80 h) and considering that the interaction between the potential hosts (nodes in the network) follows a Watts-Strogatz configuration. Note that the results clearly correspond with typical SIR curves. Fig. 2a, b and c presents, at different times, the distribution of the five hundred viral strains that compete for survival. Note that soon after the beginning of the experiment, the distribution changes dramatically, most of the viruses disappear and only a few remain to compete. At the end of the simulation (Fig. 2c), only one of the viruses survived. Fig. 2d shows the evolution of the three different populations (variables  $S, I$  and  $R$ ). As the model allows for reinfection

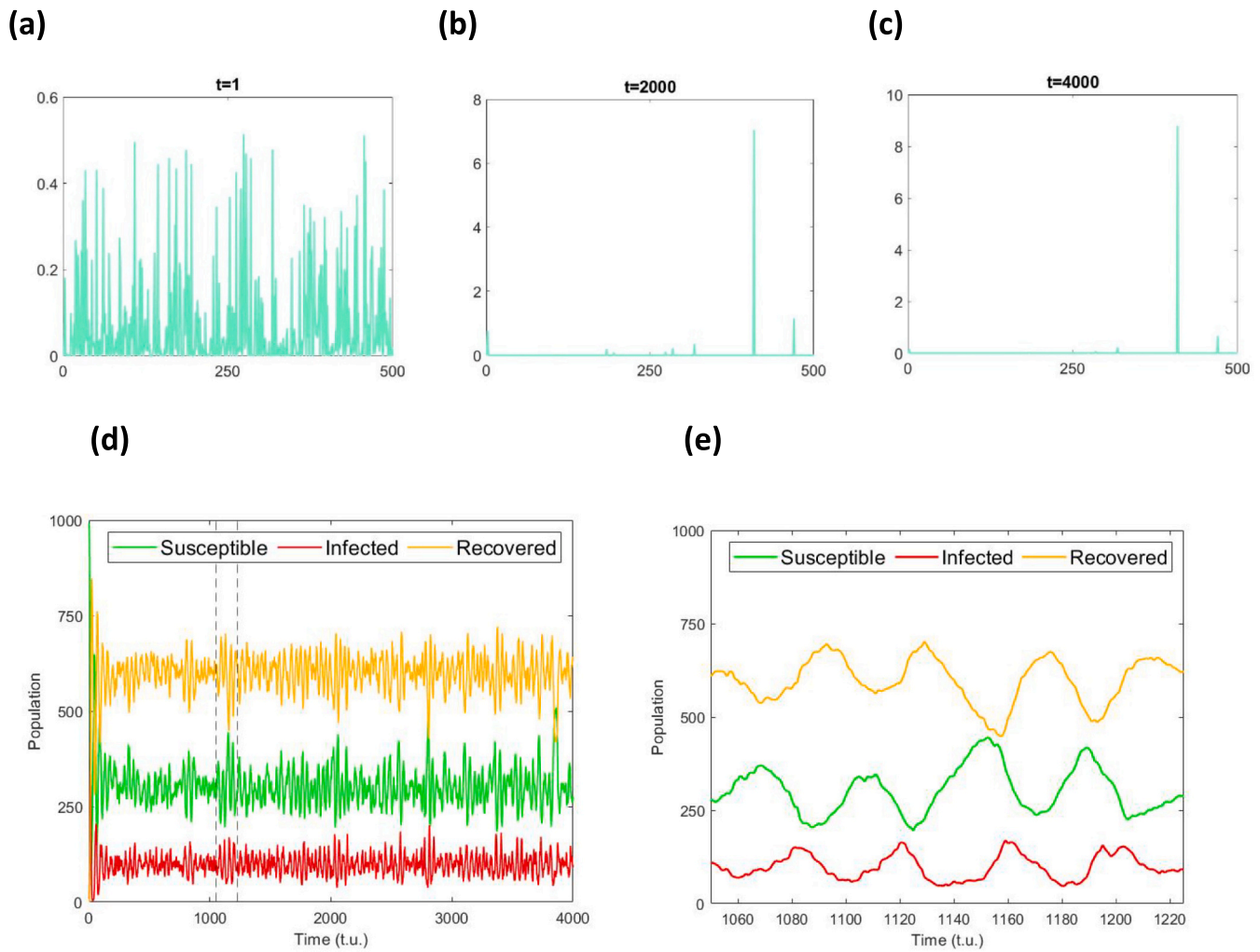


**Fig. 2.** Results of the SIR model combined with the virus competition model and a network topology for the interactions between potential hosts. (a) Distribution of viral strains at time  $t = 1 t.u.$ , (b)  $t = 2000 t.u.$  and (c) at the end of the simulation  $t = 4000 t.u.$  (d) Evolution of the SIR model variables in the same simulation. (e) Detail of the previous figure showing only four epidemic waves. The dominant virus in the strain has the following parameters:  $r = 6.2, k = 10.0, p_{inf} = 0.007, t_{sick} = 17.9$  and  $t_{reinf} = 432.7$ .

after some refractory period, an endless succession of epidemic waves goes through the system. Fig. 2e shows a zoom of these same results where four of these epidemic waves are clearly seen.

As introduced in the Methods section, three different networks are considered corresponding with completely different ways of interacting potential hosts. Examples with the three different networks are plotted in Fig. 3. Each line in Fig. 3 corresponds with a typical example of a simulation with each one of the three networks considered. The first column presents the evolution of the SIR model variables for a short period presenting only a couple of epidemic waves. The pictures to the right of each line present the spatial distribution of the SIR variables states for times corresponding with maxima and minima of the I-variable. As the epidemic model considers reinfection as a possibility for the recovered nodes, all networks exhibit consecutive waves that do not cease during the simulated intervals. Note that random and Barabasi-Albert networks do not present a spatial structure, while the Watts-Strogatz network shows some waves moving through the topology (see Supplementary Information for details). This is related to the fact that this last network is the only one that represents a physical situation where space dimension is relevant. (Animations of these examples are included in the SI.) Note that for the Watts-Strogatz network case, the epidemic wave is more intense than in the previous cases.

All simulations present a dynamic equivalent to the one presented in

Fig. 2. For each simulation and each network, the average period between epidemic waves,  $T_{wave}$ , and the time needed to reach dominance of a single virus from the strain,  $t_{fin}$ , were recorded and the results are summarized in Table 2 and Table 3 and in Fig. 4. For each simulation and each type of network, the parameters describing the final virus that survived competition among all others in the strain were recorded. Table 2 presents the values of these parameters averaged over 250 simulations. Note that in all simulations and independently of the type of interaction between potential hosts, the surviving virus is always the same (within some dispersion). The viruses with larger value of  $k$  are more prone to dominate the strain while  $r$  does not seem to be of relevance in order to achieve dominance. Table 3 presents the values of the two variables that are recorded for each simulation. These values are also plotted in Fig. 4. Fig. 4a and b present the histograms with all the values recorded, while Fig. 4c and d plot the values for each type of network of interactions. Note that  $T_{wave}$  (or period of time between consecutive epidemic waves) is clearly controlled by the type of interaction between the potential hosts. The other parameter recorded,  $t_{fin}$  (or time to reach dominance of a single virus within the strain), also presents a dependence on the type of interaction between potential hosts although the dispersion of the values is more important in this case (see Table 3).

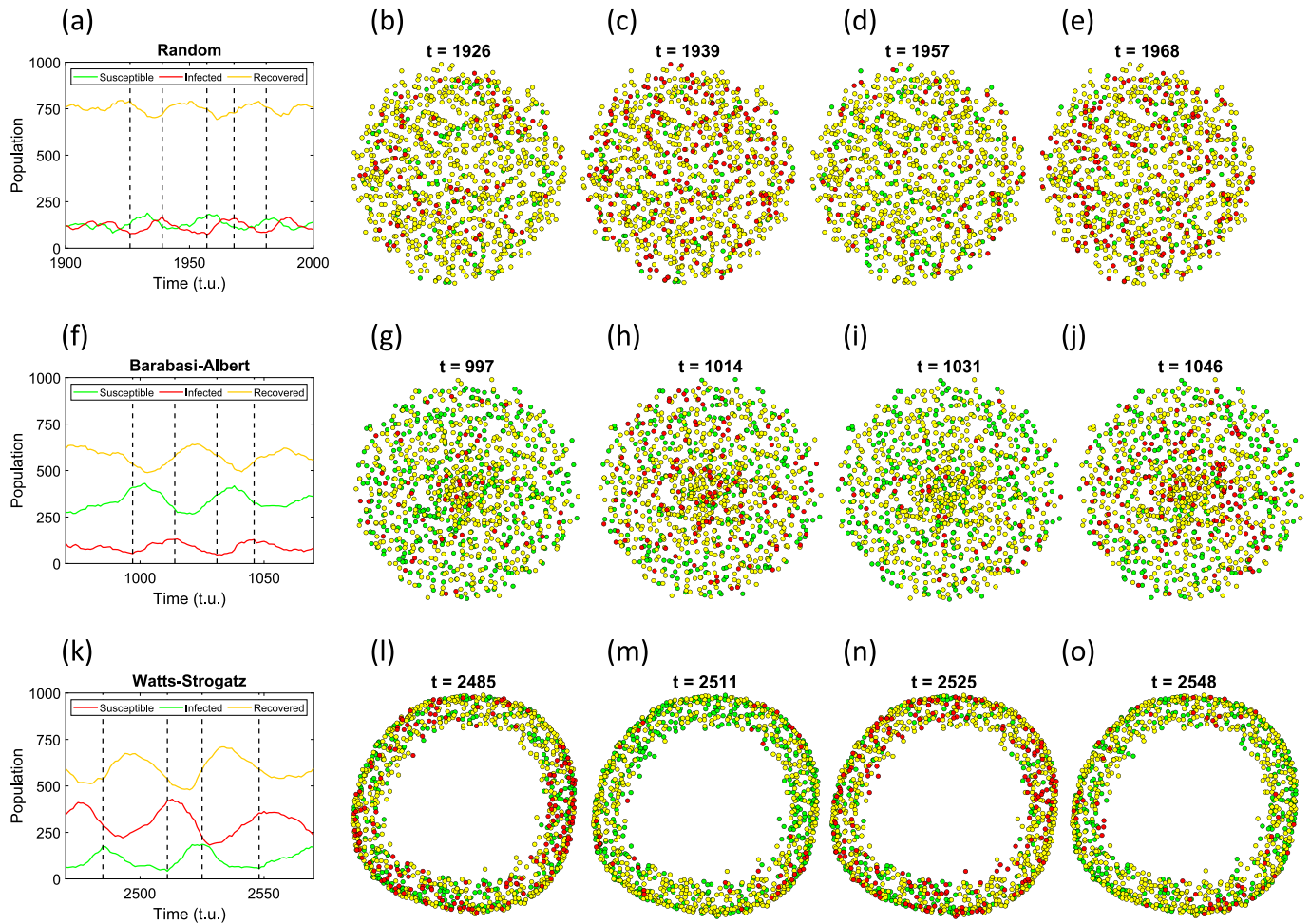


**Fig. 3.** Different network topologies affecting the disease spread. (a) Global evolution of the infection for a short period and a typical simulation considering a random network. The spatial distribution of the infected cases is shown in the consecutive figures for times: (b)  $t = 1926 t.u.$ , (c)  $t = 1939 t.u.$ , (d)  $t = 1957 t.u.$  and (e)  $t = 1968 t.u.$  Colors in the panels indicate the state of infection; green means susceptible, red infected and yellow recovered. (f) Evolution of the SIR variables for a Barabasi-Albert network. The spatial distribution of the variables is plotted in (g)  $t = 997 t.u.$ , (h)  $t = 1014 t.u.$ , (i)  $t = 1031 t.u.$  and (j)  $t = 1046 t.u.$  (k) Evolution of the SIR variables for a Watts-Strogatz network. The spatial distribution of the variables is plotted in (l)  $t = 2485 t.u.$ , (m)  $t = 2511 t.u.$ , (n)  $t = 2525 t.u.$  and (o)  $t = 2548 t.u.$  Networks are plotted using graph tools from *MATLAB* (Version R2021b) using the *UseGravity* layout so that the components are layered out radially around the origin, with more space allotted for the nodes with lower connectivity. (For interpretation of the references to colour in this figure legend, the reader is referred to the web version of this article.)

**Table 2**  
Parameters describing the surviving virus after competing with all others in the strain.

	Random network	Barabasi-Albert network	Watts-Strogatz network
$r$	$4.9 \pm 2.0$	$5.1 \pm 1.9$	$4.9 \pm 2.1$
$k$	$9.98 \pm 0.02$	$9.98 \pm 0.02$	$9.98 \pm 0.02$
$p_{inf}$	$0.005 \pm 0.002$	$0.005 \pm 0.002$	$0.004 \pm 0.002$
$t_{sick}$	$15 \pm 3$	$15 \pm 3$	$15 \pm 3$
$t_{reinf}$	$451 \pm 31$	$448 \pm 29$	$449 \pm 25$

**Table 3**  
Periodicity of the disease waves and time of dominance.

	Random network	Barabasi-Albert network	Watts-Strogatz network
$T_{wave}$	$23.8 \pm 2.9$	$32.0 \pm 3.5$	$36.8 \pm 2.8$
$t_{fin}$	$3556 \pm 1891$	$3894 \pm 2051$	$4507 \pm 2097$

#### 4. Conclusions

Along the manuscript, we constructed a minimal model that can describe the spread of a disease among a set of potential hosts. Within this context, we introduce a strain of viruses as the cause of the infection and followed at the same time the competition process among all the viruses in the strain as they trigger epidemic waves in the considered population of potential hosts. We focused on the different dynamics of interaction between the hosts and how this could be used as a control of the epidemic spread but also as a control of the virus evolution within the strain. This model effectively recovers the basic principle in Biology that only one virus survives when competing with similar ones for the same resources. In our case, the virus with larger competition rate dominates.

The effect of the network on the model proposed is twofold. First, the pandemic waves are clearly affected by the interactions network topology, being a random network the one with larger reinfection rate. It is important to note that the virus evolution itself is also affected by the network topology in the sense that the time to reach the domination of a single virus (usually the one that is more compatible with the host's life) becomes significantly increased depending on the interaction network.

In conclusion, the topology of the network, or the structure of the

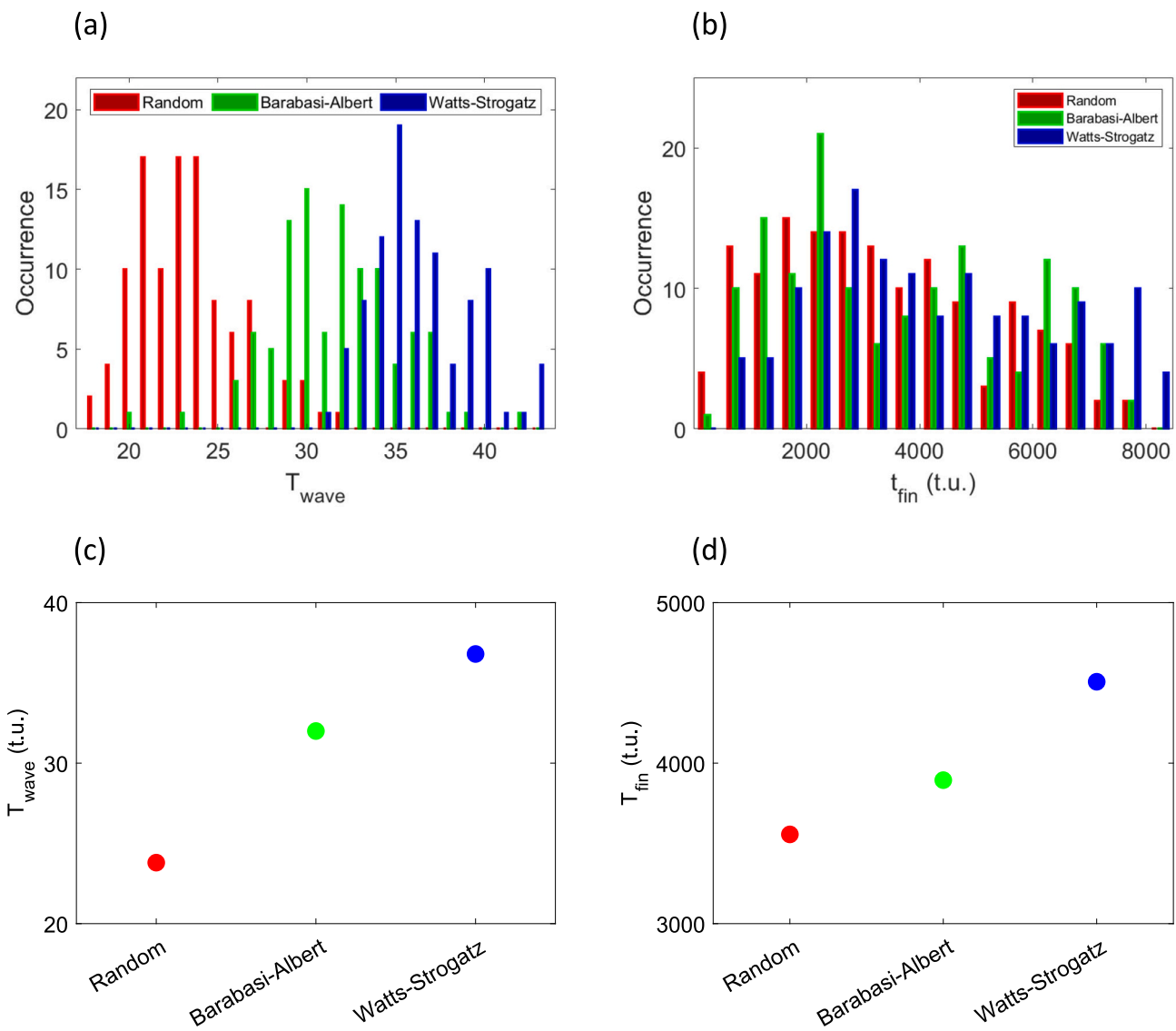


**Fig. 4.** Influence of the network topology on the pandemic and virus evolution. (a) Histogram of the pandemic wave period for the three different network topologies considered. (b) Histogram of the time needed to reach dominance of a single virus for the three different network topologies considered. (c) Variation of  $T_{wave}$  with the network topology. (d) Variation of  $t_{fin}$  with the network topology.

connections among the potential hosts, changes the behavior of the epidemic spread at both levels; the virus evolution itself and the infection propagation.

**Declaration of competing interest**

The authors declare that they have no known competing financial interests or personal relationships that could have appeared to influence the work reported in this paper.

**Data availability**

No data was used for the research described in the article.

**Acknowledgements**

We gratefully acknowledge financial support by the Spanish Ministerio de Economía y Competitividad and European Regional Development Fund under contract RTI2018-097063-B-I00 AEI/FEDER, UE, and by Xunta de Galicia under Research Grant No. 2021-PG036. All these programs are co-funded by FEDER (UE). The simulations were run in the

Supercomputer Center of Galicia (CESGA) and we acknowledge their support. EVC acknowledges financial support by Xunta de Galicia under Research Grant No. GRC GI-1563-ED431C 2021/15.

**Appendix A. Supplementary data**

Supplementary data to this article can be found online at <https://doi.org/10.1016/j.chaos.2023.113344>.

**References**

- [1] Becker RL. Breve historia de las pandemias24. *Psiquiatria. com*; 2020.
- [2] Huremović D. Brief history of pandemics (pandemics throughout history). In: *Psychiatry of pandemics*. Cham: Springer; 2019. p. 7–35.
- [3] Van Panhuis WG, Grefenstette J, Jung SY, Chok NS, Cross A, Eng H, Burke DS. Contagious diseases in the United States from 1888 to the present. *NEngJMed* 2013;369(22):2152–8.
- [4] Silva CJ, Cruz C, Torres DF, Munuzuri AP, Carballosa A, Area I, Mira J. Optimal control of the COVID-19 pandemic: controlled sanitary deconfinement in Portugal. *Sci Rep* 2021;11(1):1–15.
- [5] Carballosa A, Mussa-Juane M, Muñuzuri AP. Incorporating social opinion in the evolution of an epidemic spread. *Sci Rep* 2021;11(1):1–12.
- [6] Carballosa A, Balsa-Barreiro J, Garea A, García-Selfa D, Miramontes Á, Muñuzuri AP. Risk evaluation at municipality level of a COVID-19 outbreak

- incorporating relevant geographic data: the study case of Galicia. *Sci Rep* 2021;11(1):1–16.
- [7] Hardin G. The competitive exclusion principle: an idea that took a century to be born has implications in ecology, economics, and genetics. *Science* 1960;131(3409):1292–7.
- [8] Agarwal P., Nieto J.J., Ruzhansky M. In: Torres D.F.M., editor. *Analysis of Infectious Disease Problems (Covid-19) and Their Global Impact*. Infosys Science Foundation Series. Singapore: Springer. [https://doi.org/10.1007/978-981-16-2450-6\\_21](https://doi.org/10.1007/978-981-16-2450-6_21).
- [9] Hethcote Herbert W. The mathematics of infectious diseases. *SIAM Rev* 2000;42(4):599–653.
- [10] Grassly NC, Fraser C. Mathematical models of infectious disease transmission. *Nat Rev Microbiol* 2008;6(6):477–87.
- [11] Waltman P. *Competition models in population biology*. Society for Industrial and Applied Mathematics; 1983.
- [12] Murray JD. *Mathematical biology*. Berlin: Springer-Verlag; 1989.
- [13] Zhang X, Ruan Z, Zheng M, Zhou J, Boccaletti S, Barzel B. Epidemic spreading under mutually independent intra- and inter-host pathogen evolution. *Nat Commun* 2022;13:6218.
- [14] Barabási AL. Scale-free networks: a decade and beyond. *Science* 2009;325(5939):412–3.
- [15] Strogatz SH. Exploring complex networks. *Nature* 2001;410(6825):268–76.
- [16] Bao J, Mao X, Yin G, Yuan C. Competitive Lotka-Volterra population dynamics with jumps. *Nonlinear Anal Theory Methods Appl* 2011;74(17):6601–16.
- [17] Fabre F, Montarry J, Coville J, Senoussi R, Simon V, et al. Modelling the evolutionary dynamics of viruses within their hosts: a case study using high-throughput sequencing. *PLoS Pathog*. 2012:e1002654. <https://doi.org/10.1371/journal.ppat.1002654>.
- [18] Del Monte-Luna P, Brook BW, Zetina-Rejón MJ, Cruz-Escalona VH. The carrying capacity of ecosystems. *Glob Ecol Biogeogr* 2004;13(6):485–95.
- [19] Van Steen M. Graph theory and complex networks. *An introduction* 144; 2010.
- [20] Estrada E. *The structure of complex networks: theory and applications*. Oxford University Press; 2012.
- [21] Mata ASD. Complex networks: a mini-review. *Braz J Phys* 2020;50(5):658–72.
- [22] Huppert A, Katriel G. Mathematical modelling and prediction in infectious disease epidemiology. *Clin Microbiol Infect* 2013;19(11):999–1005.
- [23] Gomes MGM, White LJ, Medley GF. Infection, reinfection, and vaccination under suboptimal immune protection: epidemiological perspectives. *J Theor Biol* 2004; 228(4):539–49.
- [24] Diekmann O, Heesterbeek JAP. *Mathematical epidemiology of infectious diseases: model building, analysis and interpretation* Vol. 5. John Wiley & Sons; 2000.
- [25] Hethcote HW. The mathematics of infectious diseases. *SIAM Rev* 2000;42(4): 599–653.
- [26] Nowak MA, May RM. *Virus dynamics*. Oxford Univ. Press; 2000.
- [27] Kermack WO, McKendrick AG. A contribution to the mathematical theory of epidemics. In: *Proceedings of the royal society of London. Series A, Containing papers of a mathematical and physical character*. 115(772); 1927. p. 700–21.
- [28] Boccara N, Cheong K. Automata network SIR models for the spread of infectious diseases in populations of moving individuals. *J Phys A Math Gen* 1992;25(9): 2447.
- [29] Hethcote Herbert W. Three basic epidemiological models. <sb:contribution><sb: title>Appl. Math </sb:title></sb:contribution><sb:host><sb:issue><sb: series><sb:title>Ecol</sb:title></sb:series></sb:issue></sb:host> 1989;18: 119–44.
- [30] Gomes MGM, White LJ, Medley GF. Infection, reinfection, and vaccination under suboptimal immune protection: epidemiological perspectives. *J Theor Biol* 2004; 228(4):539–49.
- [31] Gomes MGM, White LJ, Medley GF. The reinfection threshold. *J Theor Biol* 2005; 236(1):111–3.
- [32] Katriel G. Epidemics with partial immunity to reinfection. *Math Biosci* 2010;228 (2):153–9.
- [33] Anderson HLMetropolis. Monte Carlo and the MANIAC. *Los Alamos Science* 1986; 14:96–108.